Spin-dependent single-electron-tunneling effects in epitaxial Fe nanoparticles

F. Ernult[a)] and K. Yamane

 Institute for Materials Research, Tohoku University, 2-1-1 Katahira, Aoba-ku, Sendai 980-8577, Japan

S. Mitani, K. Yakushiji, and K. Takanashi

 Institute for Materials Research, Tohoku University, 2-1-1 Katahira, Aoba-ku, Sendai 980-8577, Japan
 and CREST, Japan Science and Technology Agency, 4-1-8 Honchi, Kawaguchi 332-0012, Japan

Y. K. Takahashi and K. Hono

 National institute for Materials Science, 1-2-1 Sengen, Tsukuba 305-0047, Japan

 Fe/MgO/Fe nanoparticles/MgO/Co double tunnel junctions were prepared by molecular beam epitaxy for current- perpendicular-to-plane transport measurements on submicrometer-sized pillars.

Microstructural observations indicate that the samples exhibit a fully epitaxial layered structure with sharp and flat interfaces including well-defined separated Fe nanoparticles between the barriers. The introduction of asymmetric MgO tunnel barriers, i.e., with different thicknesses, in the double junction leads to a clear observation of Coulomb staircase and associated tunnel magnetoresistance oscillations. An estimation of the capacitance of the system indicates that these transport phenomena are due to charging effects of the magnetic particles. © *2004 American Institute of Physics.*

[DOI: 10.1063/1.1712035]

  In the last decade, single electron devices based on metallic or semiconductor nanoparticles sandwiched by two electrodes have attracted much attention because of their ability to control the number of electrons stored in the particles by means of the bias and/or gate voltage.[1] If magnetic materials are used for the fabrication of these devices, remarkable spin-dependent phenomena are expected due to the interplay between single electron tunneling and spin-dependent processes. The excess electrons stored in the particles cause a step-by-step increase of the current flow through the junction every time the applied voltage exceeds the charging energy $(n + 1/2)\, e^2/2C$ (where C is the capacitance of the particle and n the number of electrons in the particle). This gives rise to the so-called Coulomb staircase, characterized by a period equal to e/C. If at least two of the layers (electrodes or particles) are ferromagnetic, remarkable tunnel magnetoresistance (TMR) effects associated with the Coulomb staircase are predicted theoretically.[2-4] These effects include oscillations or enhancement of the TMR. Even though several experimental results were reported for various measurement geometries, simultaneous observation of the Coulomb staircase and TMR variation has scarcely ever been reported. The previous reports of simultaneous observation of the Coulomb staircase and associated TMR effects evidenced the difficulty of analyzing and interpreting the experimental data.

  Our previous results on 15-nm-thick CoA1O granular films in current-perpendicular-to-plane (CPP) geometry[5,6] showed clear TMR oscillations associated with the steps of the Coulomb staircase. However, the granular film contained a great number of randomly distributed magnetic particles, so that the exact number of particles between the electrodes in the current direction was not known. Furthermore, although the observation of the Coulomb staircase requires an asymmetry of the resistances on both sides of the particles, the resistances were not precisely controlled in these samples. The preparation of tunnel junctions, including a well-defined number of particles with precisely controllable barrier thickness, is essential to obtain a tunable resistance asymmetry and a model system whose results can easily be compared to the theory. In order to meet these requirements, several groups studied ferromagnetic tunnel junctions, including a single layer of nanometric particles. However, TMR oscillations were not observed[7] or could not be clearly explained.[8] Experiments designed to measure the conductance of a single nanoparticle have also been performed,[9] but the TMR was not measured. Recently, measurements of the electrical properties of self-organized Co particles in current-in-plane (CIP) geometry have been reported.[10] However, despite the narrow size distribution of the particles, Coulomb staircase and TMR oscillations were not observed, probably because of the multiple current paths between the electrodes or because of the absence of resistance asymmetry. Therefore, CPP geometry seems more suitable to observe spin-dependent single electron transport phenomena.

Appl. Phys. Lett., Vol. 84, No. 16, 19 April 2004

Ernult et al. 3107
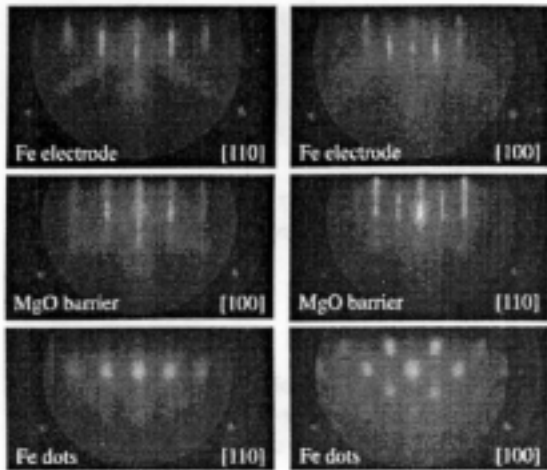
FIG. 1. RHEED patterns of a 0.5-nm-thick Fe layer deposited on a 1-nm-thick MgO tunnel barrier for the azimuths [100] and [110].

FIG. 2. (a) Schematic illustration of the structure of our samples; (b) STM image of a 0.5-nm-thick Fe layer deposited on top of a 1-nm-thick MgO barrier; (c) TEM bright-field cross section of a sample with the following structure: MgO (001)//MgO, 20 nm/Fe, 20 nm/MgO, 1 nm/Fe, 0.5 nm/MgO, 3 nm/Co, 20 nm. Inset: Corresponding selected area electron diffraction pattern along the [100] zone axis.

In the present study, we turned to molecular beam epitaxy (MBE) to achieve a good control of the structure and thickness of the different layers. MBE is also suitable for preparing flat and sharp interfaces in order to prevent any decrease of the spin polarization due to interdiffusion.

We prepared double tunnel junctions, including a single layer of Fe particles between the barriers. The current-voltage I (V) characteristics of the samples were then measured in CPP geometry after fabrication of submicrometer-sized square pillars by electron beam lithography. The samples were prepared on polished MgO (001) substrates and their structure is as follows: MgO (001)//MgO, 20 nm/Fe, 20 nm/MgO, 1 nm/Fe, t_{Fe} nm/MgO, 3 nm/Co, 20 nm [see Fig. 2(a)]. The thickness of the Fe thin layer was varied from 0.3 to 1 nm. Details on the deposition procedure of the Fe particles were published elsewhere.[11] The two MgO barriers have different thicknesses to introduce a resistance asymmetry.

The epitaxial growth of the samples is confirmed by the *in situ* reflection high energy electron diffraction (RHEED) patterns of the MgO buffer, Fe bottom electrode, and the first MgO barrier layer, all exhibiting narrow streaks characteristic of a two-dimensional 2D growth mode, as shown in Fig. 1. These RHEED patterns also indicate a MgO(001)[100]/Fe(001)[110] epitaxial relationship between the Fe bottom electrode and both the MgO buffer and MgO tunnel barrier as previously observed in studies of the growth of MgO layers on Fe buffers.[12] On the other hand, the RHEED pattern of the thin Fe layer, shown in Fig. 1, is made diffuse spots for all the deposited thicknesses, indicating a three-dimensional (3D) growth mode of bcc Fe particles. This 3D growth mode is confirmed by scanning tunneling microscopy (STM) images showing assemblies of particles. For t_{Fe} =1 nm, the percolation threshold is reached and the STM image shows elongated Fe stripes unsuitable for single

electron tunneling experiments. When the thickness is reduced to 0.5 nm and lower, the particles exhibit a quasi-circular shape. Figure 2(b) shows the STM image of the sample prepared with t_{Fe} =0.5 nm. Statistical analysis of this image allows us to estimate the size distribution of the particles, even though minor corrections to deconvolute the tip shape are needed to determine their absolute exact values. This distribution can be fitted with a log-normal law by using the following parameters: S=9.14 nm^2 and o=0.75 where S and o stand for the mean area occupied by the particles and the standard deviation of the log-normal law respectively. Assuming that the dots have a semicircular shape in the plane parallel to the interfaces, S corresponds to a mean diam of 3.4 nm. Furthermore, if we assume in a first approximation that every dot has a semispherical shape with a constant height h, then this height can be determined by comparing the deposited volume with the volume deduced from the previous fit. This leads to a mean height h=1.0 nm, indicating that the dots have pancakelike shapes with an average aspect ratio $r=h/d$ ~1/3. The density of particles has also been determined from the STM images. This density is found to be 6.5×10^{12}cm^{-2} for t_{Fe}=0.5 nm and 6.3×10^{12} cm^{-2} for t_{Fe}=0.3 nm. This almost constant density may be explained by the presence of numerous surface defects of the bottom MgO tunnel barrier acting as nucleation sites for the subsequently deposited Fe particles.[13]

The structure of the samples was also investigated by transmission electron microscopy (TEM). Figure 2(c) shows a cross-sectional TEM image of the sample prepared with t_{Fe}=0.5 nm. The light and dark contrasts basically correspond to the MgO layers and the metallic electrodes, respectively. The
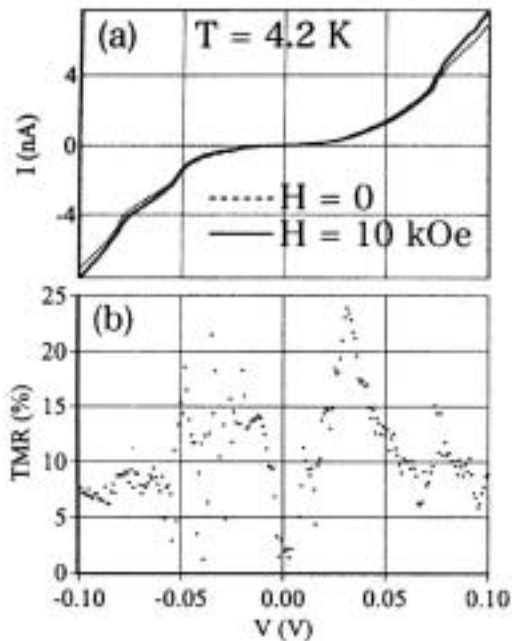
FIG. 3. (a) I(V) characteristic of the sample: MgO (001)//MgO, 20 nm/Fe, 20 nm/MgO, 1 nm/Fe, 0.5 nm/MgO, 3 nm/Co, 20 nm measured at 4.2 K; (b) corresponding TMR curve.

corresponding diffraction pattern shown in the inset of Fig. 2(c) confirms the fully epitaxial growth of the different layers. It was also confirmed from the diffraction patterns and the high-resolution cross-section images (not shown here) that the Co top electrode has a hcp structure. Furthermore, it should be emphasized that not only the interface between the Fe bottom electrode and the first MgO barrier, but also the interface between the second MgO barrier and the Co top electrode is flat in spite of its growth on the Fe islands. Therefore, the distances between the particles and both the bottom and top electrodes scarcely depend on the lateral position and the resistances of the top and bottom tunnel junctions are thought to be relatively constant throughout the whole surface of the sample. This result indicates that the ratio between the resistances of both junctions, and therefore the effect of the resistance asymmetry, can be precisely controlled by choosing adequate thicknesses of the MgO tunnel barriers.

The transport properties were measured at 4.2 K in CPP geometry after fabrication of a $0.4 \times 0.4 \mu m^2$ pillar. TMR was evaluated from the I (V) curves obtained at $H_0 = 0$ and $H_{sat} = 10$ kOe respectively. Figure 3(a) shows the $I(V)$ characteristic obtained for the sample with $t_{Fe} = 0.5$ nm. The Coulomb staircase can clearly be seen. In the positive voltage region, the first step (given by $e/2C$) occurs at a voltage of about 24 mV and the second step (given by $3e/2C$) occurs at about 74 mV. The staircase is then clearly periodic with a period of about 50 mV. The mean capacitance of the particles can be estimated to be C

=3.2 aF form this period. Figure 3(b) shows the corresponding variation of the TMR as a function of the bias voltage. TMR clearly oscillates as a function of the applied bias voltage and the positive peaks correspond to the successive steps of the Coulomb staircase. The results obtained for negative voltage exhibit noise preventing clear observation of the TMR peaks. The flatness of the interface between the two MgO barriers and the metallic electrodes, deduced from the TEM images, makes possible a rough estimation of the capacitance of the particles by using the image charge technique and by approximating the particles by spheres with an identical volume. The value obtained from these structural considerations is $C_{struc} = 1.7$ aF. This result is in good agreement with the value deduced from the period of the Coulomb staircase, thus confirming that both the staircase and the TMR oscillations are due to single electron tunneling transport through electrically isolated nanometric Fe particles.

In conclusion, fully epitaxial double tunnel junctions including nanometric particles were prepared. The sharp and flat interfaces make it possible to tune the value of the resistance asymmetry precisely. Both Coulomb staircase and oscillations of the TMR were clearly observed, and the evaluation of the capacitance of the system from structural and electrical measurements supports the fact that the observed phenomena are caused by single-electron tunneling and charging effects of the Fe particles.

1. *Single Charge Tunneling,* edited by H. Grabert and M. H. Devores (Plenum, New York, 1992).

2. J. Barnas and A. Fert, Phys. Rev. Lett. **80**, 1058 (1998).

3. I. Weymann and J. Barnas, Phys. Status Solidi **236**, 651 (2003).

4. K. Majmbar and S. Hershfield, Phys. Rev. B **57**, 11521 (1998).

5. K. Yakushiji, S. Mitani, K. Takanashi, and H. Fujimori, J. Appl. Phys. **91**, 7038 (2002).

6. S. Maelawa, S. Takahashi, and H. Imamura, *Spin dependent transport in magnetic nanostructures,* edited by S. Maekawa and T. Shinjo (Taylot & Francis, London, 2002), p. 167.

7. L. F. Schelp, A. Fert, F Fettar, P. Holody, S. F. Lee, J. L. Maurice, F. Petroff, and A. Vaurès, Phys. Rev. B **56**, R5747 (1997).

8. K. Nakajima, Y. Saito, S. Nakamura, and K. Inomata, IEEE Trans. Magn. **36**, 2806 (2000).

9. R.Desmicht, G. Faini, V. Cros, A. Fert, F. Petroff, and A. Vaurès, Appl. Phys. Lett. **72**, 386 (1998).

10. C. T. Black, C. B. Murray, R. L. Sandstrom, and S. Science **290**, 1131 (2000).

11. F.Ernult, S. Mitani, Y. Nagano, and K. Takanashi, Sci. Tech. Adv. Mat. **4**, 383 (2003).

12. J. L. Vassent, M. Dynna, A. Marty, B. Gilles, and G. Patrat, J. Appl. Phys. **80**, 5727 (1996).

13. G. Haas, A. Menck, H. Brune, J. V. Barth, J. A. Venables, and K. Kern, phys. Rev. B **61**, 11 105 (2000).